OXFORD CENTRE FOR COLLABORATIVE APPLIED MATHEMATICS

Report Number 10/40

Convection and Heat Transfer in Layered Sloping Warm-Water Aquifers

by

Robert McKibbin, Nick Hale, Robert Style and Nicole Walters

Oxford Centre for Collaborative Applied Mathematics
Mathematical Institute
24 - 29 St Giles'
Oxford
OX1 3LB
England

CONVECTION and HEAT TRANSFER in LAYERED SLOPING WARM-WATER AQUIFERS

Robert McKibbin[1]

Centre for Mathematics in Industry, Massey University, Private Bag 102 904 NSMC, Auckland, New Zealand

Nick Hale, Robert Style

Oxford Centre for Collaborative Mathematics, Mathematical Institute, Oxford, OX1 3LB, United Kingdom

Nicole Walters

School of Mathematics, Statistics and Operations Research, Victoria University of Wellington, New Zealand

Keywords: *warm-water, aquifers, convection, layered systems, mass transfer, heat transfer*

ABSTRACT

What convective flow is induced if a geologically-stratified groundwater aquifer is subject to a vertical temperature gradient? How strong is the flow? What is the nett heat transfer? Is the flow stable? How does the convection affect the subsequent species distribution if a pollutant finds its way into the aquifer? This paper begins to address such questions. Quantitative models for buoyancy-driven fluid flow in long, sloping warm-water aquifers with both smoothly- and discretely-layered structures are formulated. The steady-state profiles are calculated for the temperature and for the fluid specific volume flux (Darcy velocity) parallel to the boundaries in a sloping system subjected to a perpendicular temperature gradient, at low Rayleigh numbers. The conducted and advected heat fluxes are compared and it is shown that the system acts somewhat like a heat pipe. The maximum possible ratio of naturally advected-to-conducted heat transfer is determined, together with the corresponding permeability and thermal conductivity profiles.

[1] Corresponding author. E-mail: R.McKibbin@massey.ac.nz Fax: +64 9 441 8136

NOMENCLATURE

(SI Units given where appropriate)

A	constant [Pa m^{-1}]
c	constant (various)
c	specific heat [J kg^{-1} K^{-1}]
d	sub-layer thickness [m]
g	gravitational acceleration [m s^{-2}]
G	pressure gradient [Pa m^{-1}]
G, g, f	function (various)
H	total system thickness [m]
$\mathcal{H}$	Heaviside function
I	integral in functional
$J, \hat{J}$	functionals
k	thermal conductivity [W m^{-1} K^{-1}]
K	permeability [m^2]
N	number of sub-layers
p	fluid pressure [Pa]
P	fluid dynamic pressure [Pa]
P_n	Legendre polynomial, order n
q	specific flux [m^2 s^{-1}, W m^{-2}]
Q	dimensionless nett volume flux
Ra	Rayleigh number
t	time [s]
T	temperature [K]
u	specific fluid volume flux [m s^{-1}]
x, y, z	spatial coordinates [m]

Greek symbols

α	slope angle [radian]
β	thermal expansivity [K^{-1}]
δ	Dirac delta function
δ_{mn}	Kronecker delta function
ΔT	temperature difference [K]
ζ, ξ, θ	continuous variables
χ	dimensionless conductivity
η	dimensionless sub-layer thickness
κ	dimensionless permeability
μ	dynamic viscosity [kg m^{-1} s^{-1}]
ν	kinematic viscosity [m^2 s^{-1}]
ξ, η	permeability, conductivity anisotropy
ρ	density [kg m^{-3}]
ϕ	porosity [–]

Subscripts

$\perp$	perpendicular to bedding plane
$\rightleftharpoons$	natural circulation
$=$	parallel to bedding plane
0	datum value at axes origin
a	datum value at upper boundary
crit	critical value
f	fluid
h	heat
i, j, r	layer numbers
m	matrix-fluid mixture value
m, n	layer numbers
P	at constant pressure
r	ratio
s	solid matrix
SS	steady state

Superscripts

$\bar{}$	(overbar) weighted average
*	special value (as defined in text)

1. INTRODUCTION

1.1 Thermally-driven convection

Thermal convection in porous media has been extensively studied in a variety of settings and applications, and is reviewed in comprehensive fashion by Nield & Bejan (2006). The criterion for onset of convection in a layer that is heated from below has been the subject of many publications since the work by Horton & Rogers (1945) and Lapwood (1948). The motionless equilibrium state of a saturated permeable layer may be stable to thermal gradients in special cases (horizontal layer, uniform temperature horizontal boundaries, small enough Rayleigh number, etc.); however, any thermal non-uniformity either on the boundaries or heat sources usually provides conditions for convective motion. In particular, non-horizontal heated boundaries immediately provide thermal buoyancy forces that drive the fluid.

Convection in sloping permeable layers has been studied by Ludvigsen *et al.* (1992) and Trew & McKibbin (1994), amongst others. Both considered multi-layered systems subjected to uniform vertical salinity and/or temperature gradients. Provided the system Rayleigh number Ra is not too large in a homogeneous system ($\mathrm{Ra} < 4\pi^2 \cos\alpha$, where α is the layer slope angle), a steady stable unicellular convection cell may be established (Bories & Combarnous, 1973; Caltagirone & Bories, 1985; Ludvigsen *et al*., 1992; Mullis, 1995), and the flow far from the ends of a system with a small thickness-to-length ratio will be parallel to the upper and lower boundaries.

This paper provides quantification of such convective motion induced by temperature differences across a sloping porous slab of finite thickness. The heat flow is dominated by conduction, but a small-scale convective motion is induced. Under the conditions described above, this motion is a flow parallel to the sloping boundaries. A model is formulated here for the case where the aquifer system has a layered structure, smooth or discrete, due to geological bedding. Continuous variation in matrix properties through the layer may also be treated using the discrete model, by dividing the system into sub-layers within each of which the matrix properties are constant.

1.2 Model formulation

First, the equations that describe the movement of the fluid and thermal energy are summarized. Secondly, steady-state fluid flow and temperature profiles due to natural convection are found for a sloping system. The system is somewhat analogous to a heat pipe; here there is an up-slope nett heat flux parallel to the plane of layering. Using the steady-state profiles, the nett sensible advected heat is calculated and compared with the heat conducted across the layer. This ratio

depends on the thermal conductivity and permeability structure of the system. Finally, the profiles of these properties that maximize the ratio are found.

The technique of using a layered model, either in its own right or as an approximate analogue of a continuous system, has been explored in other contexts. For example, McKibbin & O'Sullivan (1981) and McKibbin (1992) investigated thermally-driven convection in horizontal layered porous media. McKibbin & Tyvand (1982) studied the correspondence between layering and anisotropy and how the results for either one could inform those for the other. Lim *et al*. (2008) and McKibbin (2008), using Green functions, found analytic expressions for the airborne concentration and ground deposits of volcanic ash that falls though a stratified atmosphere.

Because, in general, quantitative modelling of the dispersion of a pollutant or tracer in a non-homogeneous system requires numerical simulation of the whole domain, any discretisation that saves computational time is useful; see McKibbin (2009) for example. The aim here is to use the natural bedded structure of such geological systems to advantage; for discrete layering, layer-averaged quantities are used. The results of this model should be applicable to analyzing fluid fluxes and temperature profiles occurring in sloping aquifers. It is worth noting that most aquifers have some degree of tilt caused by crustal movement after a sequence of alluvial layers are deposited. Use of this model may enable quantification of resulting natural flows.

2. THE EQUATIONS FOR FLUID AND HEAT FLOW

Consider thermally-driven convection of a fluid (considered here to be a liquid) within a sloping porous layer of uniform total thickness *H*, bounded above and below by impervious surfaces. The (planar) upper boundary is maintained at temperature T_a while the bottom boundary is kept at the higher temperature $T_a + \Delta T$. Cartesian coordinates (x, y, z) are aligned so that the positive *x*-axis points (upwards) along the base of the sloping layer in the direction of greatest slope (angle $\alpha \geq 0$ to the horizontal), with the gravitational acceleration vector given by $\underset{\sim}{g} = (-g\sin\alpha, 0, -g\cos\alpha)$.

The layer lies between the hotter bottom boundary at $z = 0$ and the cooler top surface at $z = H$. The matrix parameters may vary through the thickness of the layer. The equations describing conservation of mass, momentum and energy of the fluid within the layer are [see Nield & Bejan (2006), for example]:

$$\phi \frac{\partial \rho_f}{\partial t} = -\nabla \cdot (\rho_f \underset{\sim}{u})$$
$$\underset{\sim}{u} = \frac{K}{\mu_f}(-\nabla p + \rho_f \underset{\sim}{g}) \qquad (1)$$
$$(\rho c)_m \frac{\partial T}{\partial t} = -\nabla \cdot \left[(\rho c_P)_f T \underset{\sim}{u} - k_m \nabla T \right]$$

Here, ϕ [dimensionless] is the matrix porosity, T [K] is the temperature, $\rho_f(T)$ [kg m^{-3}] is the fluid density, $\underset{\sim}{u}$ [(m^3 s^{-1}) m^{-2} = m s^{-1}] is the specific fluid volume flux (usually termed the Darcy velocity), $K(z)$ [m^2] is the matrix permeability (assumed to be locally isotropic), $\mu_f(T)$ [kg m^{-1} s^{-1}] is the dynamic viscosity of the fluid and p [Pa = kg m^{-1} s^{-2}] is the fluid pressure.

The specific heat content $(\rho c)_m$ and the thermal conductivity k_m of the fluid-saturated medium (a matrix-fluid "mixture"), both subscripted *m*, may be found by suitably-weighted combinations of the solid matrix (subscript *s*) and fluid parameters (subscripted *f*). For example [see Nield & Bejan (2006)]:

$$(\rho c)_m = (1-\phi)(\rho c)_s + \phi(\rho c_P)_f$$
$$k_m = (1-\phi)k_s + \phi k_f$$

Here, $c_p(T)$ [J kg^{-1} K^{-1}] is the specific heat of the fluid and $k_m(z)$ [W m^{-1} K^{-1}] is the (locally isotropic) thermal conductivity of the fluid-saturated porous medium.

Invoking the Boussinesq approximation, the density variation (due to thermal expansion) of the fluid is neglected except in the momentum equation (Darcy's Law), where it is approximated by $\rho_f = \rho_a[1-\beta(T-T_a)]$ with $\rho_a = \rho_f(T_a)$ [kg m^{-3}], where T_a is the (reference) upper boundary temperature, and β [K^{-1}] is the fluid thermal expansivity; elsewhere, $\rho_f = \rho_a$. [This means that $\nabla \cdot \underset{\sim}{u} = 0$ (the model velocity field is solenoidal).] Likewise, the fluid's dynamic viscosity, $\mu_a = \mu_f(T_a)$ and its specific heat $c_a = c_P(T_a)$ are both assumed constant throughout the system.

2.1 Natural steady-state flow in a sloping system

When the sloping porous layer has matrix parameters that vary only in the *z*-direction, the relevant equations for a steady flow $\underset{\sim}{u} = (u_{SS}(z), 0, 0)$ parallel to the boundaries, under the influence of temperature distribution $T_{SS}(z)$ and the corresponding pressure $p_{SS}(x,z)$, are, from (1):

$$\frac{\partial p_{SS}}{\partial x} = -\rho_a\{1-\beta[T_{SS}(z)-T_a]\}g\sin\alpha - \frac{\mu_a}{K(z)}u_{SS}(z)$$

$$\frac{\partial p_{SS}}{\partial z} = -\rho_a\{1-\beta[T_{SS}(z)-T_a]\}g\cos\alpha \qquad (2)$$

$$\frac{d}{dz}\left(k_m(z)\frac{dT_{SS}}{dz}\right) = 0$$

The temperature boundary conditions are:

$$T_{SS}(0) = T_a + \Delta T,\ \ T_{SS}(H) = T_a \qquad (3)$$

Note that such a fluid flow automatically satisfies the equation of conservation of mass in (1). Integration of the third (energy) equation in (2) and use of the thermal boundary conditions gives:

$$T_{SS}(z) = T_a + \frac{\bar{k}_{m\perp}\Delta T}{H}\int_z^H \frac{d\zeta}{k_m(\zeta)} \qquad (4)$$

where $\bar{k}_{m\perp}$ is the mean thermal conductivity of the aquifer perpendicular to the bedding plane, defined by:

$$\int_0^H \frac{dz}{k_m(z)} = \frac{H}{\bar{k}_{m\perp}} \qquad (5)$$

Substitution of (4) into the second equation of (2), followed by integration w.r.t. z, gives:

$$p_{SS}(x,z) = P_{SS}(x) - \rho_a g\cos\alpha z + \rho_a\beta\Delta T g\cos\alpha\frac{\bar{k}_{m\perp}}{H}\int_0^z\left(\int_\xi^H \frac{d\zeta}{k_m(\zeta)}\right)d\xi \qquad (6)$$

where $P_{SS}(x) = p_{SS}(x,0)$ is to be determined. Substitution of (6) into the first equation of (2) then gives:

$$\frac{dP_{SS}}{dx} = -\rho_a g\sin\alpha + \rho_a\beta\Delta T g\sin\alpha\frac{\bar{k}_{m\perp}}{H}\int_z^H \frac{d\zeta}{k_m(\zeta)} - \frac{\mu_a}{K(z)}u_{SS}(z) \qquad (7)$$

Since the LHS is a function of x only, and the RHS is a function of z only, both must be constant. Setting $dP_{SS}/dx = -A$ [Pa m^{-1}], say, then:

$$u_{SS}(z) = \frac{A-\rho_a g\sin\alpha}{\mu_a}K(z) + \frac{\rho_a\beta\Delta T g\sin\alpha}{\mu_a}K(z)\frac{\bar{k}_{m\perp}}{H}\int_z^H \frac{d\zeta}{k_m(\zeta)} \qquad (8)$$

where the constant A may be found in terms of the nett (total) volume flux per unit aquifer width q_{SS} [$(\mathrm{m}^3\ \mathrm{s}^{-1})\ \mathrm{m}^{-1} = \mathrm{m}^2\ \mathrm{s}^{-1}$] parallel to the layers, i.e.,

$$q_{SS} = \int_0^H u_{SS}(z)dz = \frac{A - \rho_a g \sin\alpha}{\mu_a} H\bar{K}_{=} + \frac{\rho_a \beta \Delta T g \sin\alpha}{\mu_a} \frac{\bar{k}_{m\perp}}{H} \int_0^H K(\xi)\left(\int_\xi^H \frac{d\zeta}{k_m(\zeta)} \right) d\xi \tag{9}$$

Here, $\bar{K}_{=}$ is the mean permeability of the aquifer parallel to the bedding plane, defined by:

$$\int_0^H K(z)dz = H\bar{K}_{=} \tag{10}$$

Rearrangement of (9) allows A to be written in the form:

$$A = G + \rho_a g \sin\alpha - \rho_a \beta \Delta T g \sin\alpha \ \frac{\bar{k}_{m\perp}}{H^2 \bar{K}_{=}} \int_0^H K(\xi)\left(\int_\xi^H \frac{d\zeta}{k_m(\zeta)} \right) d\xi \tag{11}$$

where $G = (\mu_a / H\bar{K}_{=}) q_{SS}$ is the applied pressure gradient in the x-direction such that $G = 0$ produces a zero net volume flux through the system. Therefore natural convection corresponds to the case $q_{SS} = 0$. The x-component of the Darcy velocity is:

$$u_{SS}(z) = \frac{K(z)}{H\bar{K}_{=}} q_{SS} + \frac{\rho_a \beta \Delta T g}{H^2 \mu_a} \sin\alpha \ K(z) \left\{ H\bar{k}_{m\perp} \int_z^H \frac{d\zeta}{k_m(\zeta)} - \frac{\bar{k}_{m\perp}}{\bar{K}_{=}} \int_0^H K(\xi)\left(\int_\xi^H \frac{d\zeta}{k_m(\zeta)} \right) d\xi \right\} \tag{12}$$

with a corresponding pressure distribution given by:

$$\begin{aligned} p_{SS}(x,z) = {} & p_0 - \rho_a g \sin\alpha x - \rho_a g \cos\alpha z - \frac{\mu_a}{H\bar{K}_{=}} q_{SS} x \\ & + \rho_a \beta \Delta T g \left\{ \sin\alpha \ x \ \frac{\bar{k}_{m\perp}}{H^2 \bar{K}_{=}} \int_0^H K(\xi)\left(\int_\xi^H \frac{d\zeta}{k_m(\zeta)} \right) d\xi + \cos\alpha \frac{\bar{k}_{m\perp}}{H} \int_0^z \left(\int_\xi^H \frac{d\zeta}{k_m(\zeta)} \right) d\xi \right\} \end{aligned} \tag{13}$$

where $p_0 = p_{SS}(0,0)$. Note that if the system is horizontal ($\alpha = 0$):

$$\begin{aligned} T_{SS}(z) &= T_a + \Delta T \frac{\bar{k}_{m\perp}}{H} \int_z^H \frac{d\zeta}{k_m(\zeta)} \\ u_{SS}(z) &= \frac{K(z)}{H\bar{K}_{=}} q_{SS} \\ p_{SS}(x,z) &= p_0 - \frac{\mu_a}{H\bar{K}_{=}} q_{SS} x - \rho_a g z + \rho_a \beta \Delta T g \frac{\bar{k}_{m\perp}}{H} \int_0^z \left(\int_\xi^H \frac{d\zeta}{k_m(\zeta)} \right) d\xi \end{aligned} \tag{14}$$

If $q_{SS} = 0$, this is a motionless state; the vertical pressure distribution is hydrostatic. For $q_{SS} \neq 0$, the temperature distribution remains as above, but the pressure distribution in the longitudinal direction is altered.

2.2 Uniform matrix

In general, if the permeability $K(z)$ is uniform [i.e. $K(z) = \bar{K}_{=} = K$, a constant], then:

$$u_{SS}(z) = \frac{q_{SS}}{H} + \frac{\rho_a \beta g K}{H \mu_a} \sin\alpha \left\{ H[T_{SS}(z) - T_a] - \int_0^H [T_{SS}(\zeta) - T_a] d\zeta \right\} \tag{15}$$

It may be seen from the last expression that continuity of $T_{SS}(z)$ implies that $u_{SS}(z)$ is also continuous, as would be expected. In general, any discontinuities in $u_{SS}(z)$ are due to those in the permeability $K(z)$ (see further below). In summary, when the matrix is homogeneous,

$$\begin{aligned} T_{SS}(z) &= T_a + \Delta T \left(1 - \frac{z}{H} \right) \\ u_{SS}(z) &= \frac{q_{SS}}{H} + \frac{\rho_a \beta \Delta T g K}{\mu_a} \sin\alpha \left(\frac{1}{2} - \frac{z}{H} \right) \\ p_{SS}(x,z) &= p_0 - \left[\rho_a g \sin\alpha \left(1 - \frac{1}{2} \beta \Delta T \right) + \frac{\mu_a}{KH} q_{SS} \right] x - \rho_a g \cos\alpha \left[z - \beta \Delta T \left(z - \frac{z^2}{2H} \right) \right] \end{aligned} \tag{16}$$

Note that these formulae are all independent of the (uniform) thermal conductivity of the fluid-saturated matrix.

2.3 Layered system

For the case of a system that is composed of N distinct, separately-homogeneous sub-layers, where Layer j, occupying $z_{j-1} < z < z_j$, has thickness $d_j = z_j - z_{j-1}$ (where $z_0 = 0$ and $z_N = H$), permeability K_j, thermal conductivity k_{mj}, and mixture specific heat content $(\rho c)_{mj}$, $j = 1, 2, \ldots, N$, the steady-state temperature profile is given in that layer by

$$T_{SSj}(z) = T_a + \Delta T \left[1 - \frac{\bar{k}_{m\perp}}{H} \left(\sum_{i=1}^{j-1} \frac{d_i}{k_{mi}} + \frac{z - z_{j-1}}{k_{mj}} \right) \right] \tag{17}$$

while the fluid flux profile is:

$$u_{SSj}(z) = \frac{K_j}{H\bar{K}_=} q_{SS} + \frac{\rho_a \beta \Delta T g}{\mu_a} \sin\alpha \; K_j \left\{ \frac{\bar{k}_{m\perp}}{H^2 \bar{K}_=} \sum_{r=1}^{N} \left[d_r K_r \left(\sum_{i=1}^{r-1} \frac{d_i}{k_{mi}} + \frac{d_r}{2k_{mr}} \right) \right] - \frac{\bar{k}_{m\perp}}{H} \left(\sum_{i=1}^{j-1} \frac{d_i}{k_{mi}} + \frac{z - z_{j-1}}{k_{mj}} \right) \right\} \tag{18}$$

where the mean parallel permeability and perpendicular thermal conductivity for the aquifer are defined by:

$$\bar{K}_= = \frac{1}{H} \sum_{i=1}^{N} d_i K_i = \sum_{i=1}^{N} \frac{d_i}{H} K_i, \qquad \frac{1}{\bar{k}_{m\perp}} = \frac{1}{H} \sum_{i=1}^{N} \frac{d_i}{k_{mi}} = \sum_{i=1}^{N} \frac{d_i}{H} \frac{1}{k_{mi}} \tag{19}$$

The temperature and flux profiles may be written, for $z_{j-1} < z < z_j$, in the form:

$$T_{SSj}(z) = T_a + \Delta T \left[1 - \left(\sum_{i=1}^{j-1} \frac{\eta_i}{\chi_i} + \frac{(z - z_{j-1})/H}{\chi_j} \right) \right] \tag{20}$$

$$u_{SSj}(z) = \kappa_j \frac{q_{SS}}{H} + \frac{\rho_a \beta \Delta T g \bar{K}_=}{\mu_a} \sin\alpha \; \kappa_j \left\{ \sum_{r=1}^{N} \left[\eta_r \kappa_r \left(\sum_{i=1}^{r-1} \frac{\eta_i}{\chi_i} + \frac{\eta_r}{2\chi_r} \right) \right] - \left(\sum_{i=1}^{j-1} \frac{\eta_i}{\chi_i} + \frac{(z - z_{j-1})/H}{\chi_j} \right) \right\} \tag{21}$$

where $\eta_j = d_j / H$, $\kappa_j = K_j / \bar{K}_=$, $\chi_j = k_{mj} / \bar{k}_{m\perp}$, with

$$\sum_{j=1}^{N} \eta_j = \sum_{j=1}^{N} \eta_j \kappa_j = \sum_{j=1}^{N} \eta_j / \chi_j = 1 . \tag{22}$$

The mean volume flux in Layer *j* is given by $\bar{u}_{SSj} = \frac{1}{d_j} \int_{z_{j-1}}^{z_j} u_{SSj}(z) dz$. In non-dimensionalised form:

$$\frac{\bar{u}_{SSj}}{\mu_a^{-1} \rho_a \beta \Delta T g \bar{K}_=} = \kappa_j \left[\left[Q + \sin\alpha \left\{ \sum_{r=1}^{N} \left[\eta_r \kappa_r \left(\sum_{i=1}^{r-1} \frac{\eta_i}{\chi_i} + \frac{\eta_r}{2\chi_r} \right) \right] - \left(\sum_{i=1}^{j-1} \frac{\eta_i}{\chi_i} + \frac{\eta_j}{2\chi_j} \right) \right\} \right] \right] \tag{23}$$

where $Q = \frac{\mu_a}{H \rho_a \beta \Delta T g \bar{K}_=} q_{SS}$ is the dimensionless nett volume flux. Note that $\sum_{j=1}^{N} \eta_j \bar{u}_{SSj} = q_{SS}$.

The temperature and volume flux profiles are piecewise linear; the temperature is continuous, while the volume flux is discontinuous wherever the matrix permeability is discontinuous. Figure 1 shows an example of the profiles of the dimensionless temperature $[T_{SS}(z) - T_a]/\Delta T$ and specific volume flux $\left[u_{SS}(z)/\left(\mu_a^{-1}\rho_a\beta\Delta T g\bar{K}_=\right)\right]/\sin\alpha$ for the case where an aquifer of total thickness H is divided into $N = 5$ layers with parameters as listed in Table 1, for slope angle $\alpha > 0$ and net flux $q_{SS} = 0$. Profiles for a homogeneous system ($N = 1, \bar{K}_= = K$) are illustrated in Figure 2. Note that in both cases, $q_{SS} = \int_0^H u_{SS}(z)dz = 0$.

When there is a net throughflow caused by an excess longitudinal pressure gradient G, the velocity profiles are altered. An example is shown in Figure 3, where the dimensionless temperature and volume flux profiles are shown for the same parameters as in Table 1, but with $Q/\sin\alpha = 1$, $\alpha > 0$. Note that the temperature profile is the same as for Figure 1.

Table 1. Matrix parameters for a 5-layer system.
The steady-state temperature and flux profiles are shown in
Figure 1 (where net flux $q_{SS} = 0$) and Figure 3 (where $Q/\sin\alpha = 1$, $\alpha > 0$).

Layer	$\eta_j = d_j/H$	$\kappa_j = K_j/\bar{K}_=$	$\chi_j = k_{mj}/\bar{k}_{m\perp}$
1	0.2	1.0	0.5
2	0.2	0.5	2.0
3	0.2	2.0	0.75
4	0.2	0.8	2.0
5	0.2	0.7	1.5

In Figures 1– 3, the mean layer specific volume fluxes are marked with dashed lines. In Figure 2, these illustrate the case where a homogeneous layer is discretised into 10 sub-layers of equal thickness.

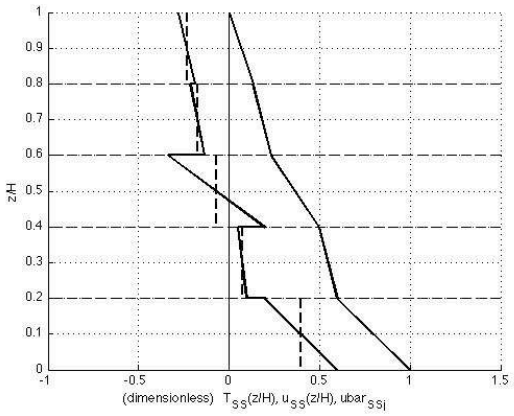

Figure 1. Scaled profiles of steady-state temperature (solid continuous line), volume flux (solid discontinuous) and mean layer volume fluxes (dashed) in a sloping aquifer composed of 5 layers whose matrix properties are listed in Table 1. There is zero net flux, i.e., $q_{SS} = 0$.

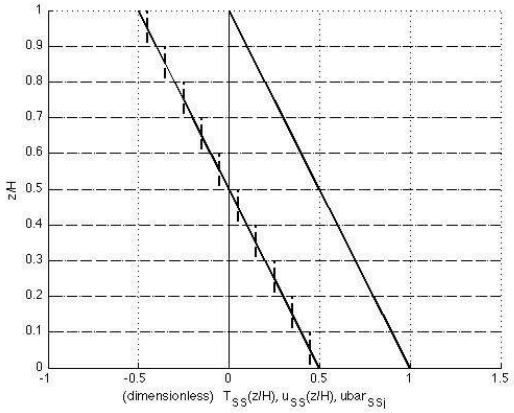

Figure 2. Scaled profiles of steady-state temperature (solid line, right) and volume flux (solid, left) and mean layer volume fluxes (dashed) in a homogeneous sloping aquifer where there is zero net flux, i.e., $q_{SS} = 0$.

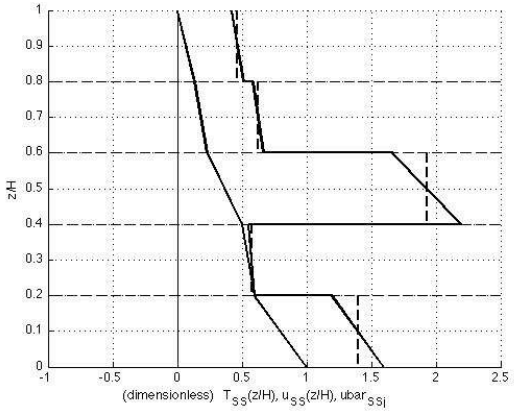

Figure 3. Scaled profiles of steady-state temperature (solid continuous line), volume flux (solid discontinuous) and mean layer volume fluxes (dashed) in a sloping aquifer composed of 5 layers whose matrix properties are listed in Table 1. The net flux in this example is related to the angle by $Q/\sin\alpha = 1,\ \alpha > 0$.

3. HEAT TRANSFER

The heat flux per unit area in the system [W m^{-2}] is:

$$\underset{\sim}{q}_h = \rho_f c_f T \underset{\sim}{u} - k_m \nabla T \tag{24}$$

With $\underset{\sim}{u} = (u_{SS}(z), 0, 0)$ and $T = T_{SS}(z)$, and use of the Boussinesq approximation, this becomes

$$\underset{\sim}{q}_h = \left(\rho_a c_a T_{SS}(z) u_{SS}(z), 0, -k_m(z) \frac{dT_{SS}}{dz} \right) \tag{25}$$

It is composed of two parts:

• uniform constant conducted heat flux $q_{h\perp} = -k_m(z) \dfrac{dT_{SS}}{dz}$ [W m^{-2}] from the constant-temperature bottom boundary to the cooler upper boundary [see (2)];

• advected sensible heat flux $q_{h=}(z) = \rho_a c_a [T_{SS}(z) - T_a] u_{SS}(z)$ [W m^{-2}] (with reference to datum temperature $T = T_a$) in the longitudinal direction of the aquifer system. This varies with depth, but a (constant) total averaged value can be found from:

$$\overline{q}_{h=} = \frac{1}{H} \int_0^H \rho_a c_a [T_{SS}(z) - T_a] u_{SS}(z) dz \tag{26}$$

3.1 Homogeneous aquifer

From Equation (16),

$$T_{SS}(z) = T_a + \Delta T \left(1 - \frac{z}{H} \right) \quad \text{and} \quad u_{SS}(z) = \frac{q_{SS}}{H} + \frac{\rho_a \beta \Delta T g K}{\mu_a} \sin\alpha \left(\frac{1}{2} - \frac{z}{H} \right) \tag{27}$$

Then the components of the heat flux are:

$$q_{h\perp} = k_m \frac{\Delta T}{H} \quad \text{and} \quad \overline{q}_{h=} = \frac{\rho_a c_a \Delta T}{2H} q_{SS} + \Delta T \frac{\rho_a c_a \beta \Delta T g K}{12 \nu_a} \sin\alpha \tag{28}$$

where $\nu_a = \mu_a / \rho_a$ [m^2 s^{-1}] is the kinematic viscosity of the fluid. The dimensionless ratio of the advected heat flux to the conducted flux is:

$$q_{hr} = \frac{\bar{q}_{h=}}{q_{h\perp}} = \frac{\rho_a c_a}{2k_m} q_{SS} + \frac{1}{12} \frac{\rho_a c_a \beta \Delta T g K H}{\nu_a k_m} \sin\alpha \tag{29}$$

The component of the longitudinal heat flux due to the natural circulation is found, by setting $q_{SS} = 0$, to be:

$$\bar{q}_{h\rightleftharpoons} = \frac{\Delta T}{H} \frac{\rho_a c_a \beta \Delta T g K H}{12 \nu_a} \sin\alpha \tag{30}$$

The ratio of this component to that through the boundaries is

$$\frac{\bar{q}_{h\rightleftharpoons}}{q_{h\perp}} = \frac{1}{12} \frac{\rho_a c_a \beta \Delta T g K H}{\nu_a k_m} \sin\alpha = \frac{1}{12} \mathrm{Ra} \sin\alpha \tag{31}$$

where $\mathrm{Ra} = \dfrac{\rho_a c_a \beta \Delta T g K H}{\nu_a k_m}$ is the Rayleigh number for the system. While Ra is small here, this ratio is also small; nevertheless, the naturally convective system acts like a heat pipe, with greater heat flow up the aquifer slope than down, even though in the pure counterflow case, the net fluid flux q_{SS} is zero.

3.2 Horizontal system

If the system is horizontal ($\alpha = 0$), Equation (14) gives:

$$T_{SS}(z) = T_a + \Delta T \frac{\bar{k}_{m\perp}}{H} \int_z^H \frac{d\zeta}{k_m(\zeta)} \quad \text{and} \quad u_{SS}(z) = \frac{K(z)}{H \bar{K}_=} q_{SS} \tag{32}$$

Then,

$$\begin{aligned} q_{h\perp} &= \bar{k}_{m\perp} \frac{\Delta T}{H} \\ \bar{q}_{h=} &= = \frac{\rho_a c_a \Delta T \bar{k}_{m\perp}}{H^3 \bar{K}_=} \left[\int_0^H K(z) \left(\int_z^H \frac{d\zeta}{k_m(\zeta)} \right) dz \right] q_{SS} \end{aligned} \tag{33}$$

and the ratio of the longitudinal advected heat flux to the through-aquifer conducted heat flux is:

$$q_{hr} = \frac{\bar{q}_{h=}}{q_{h\perp}} = \frac{\rho_a c_a}{H^2 \bar{K}_=} \left[\int_0^H K(z) \left(\int_z^H \frac{d\zeta}{k_m(\zeta)} \right) dz \right] q_{SS} \tag{34}$$

Note that when K and k_m are constant,

$$q_{hr} = \frac{\bar{q}_{h=}}{q_{h\perp}} = \frac{\rho_a c_a}{2k_m}\, q_{SS} \tag{35}$$

as in (29) with $\alpha = 0$. So, in the horizontal case, all advective heat transfer is driven by forced flow in the system, with no natural convection, as expected.

3.3 General case

In the general case, (4) and (13) give:

$$\begin{aligned} T_{SS}(z) &= T_a + \frac{\bar{k}_{m\perp}\Delta T}{H}\int_z^H \frac{d\zeta}{k_m(\zeta)} \\ u_{SS}(z) &= \frac{K(z)}{H\bar{K}_=} q_{SS} + \frac{\rho_a \beta \Delta T g}{H^2 \mu_a}\sin\alpha\; K(z)\left\{ H\bar{k}_{m\perp}\int_z^H \frac{d\zeta}{k_m(\zeta)} - \frac{\bar{k}_{m\perp}}{\bar{K}_=}\int_0^H K(\xi)\left(\int_\xi^H \frac{d\zeta}{k_m(\zeta)}\right)d\xi \right\} \end{aligned} \tag{36}$$

Then the conducted and average advected heat fluxes are given by

$$\begin{aligned} q_{h\perp} &= \bar{k}_{m\perp}\frac{\Delta T}{H} \\ \bar{q}_{h=} &= \bar{k}_{m\perp}\frac{\Delta T}{H}\frac{\rho_a c_a q_{SS}}{\bar{k}_{m\perp}}\left[\frac{1}{H}\int_0^H \frac{K(z)}{\bar{K}_=}\left(\frac{1}{H}\int_z^H \frac{\bar{k}_{m\perp}d\zeta}{k_m(\zeta)}\right)dz\right] \\ &\quad + \bar{k}_{m\perp}\frac{\Delta T}{H^2}\overline{\mathrm{Ra}}^*\sin\alpha\int_0^H \left\{\frac{K(z)}{\bar{K}_=}\left(\frac{1}{H}\int_z^H \frac{\bar{k}_{m\perp}d\zeta}{k_m(\zeta)}\right)\left[\frac{1}{H}\int_z^H \frac{\bar{k}_{m\perp}d\zeta}{k_m(\zeta)} - \frac{1}{H}\int_0^H \frac{K(\xi)}{\bar{K}_=}\left(\frac{1}{H}\int_\xi^H \frac{\bar{k}_{m\perp}d\zeta}{k_m(\zeta)}\right)d\xi\right]\right\}dz \end{aligned}$$

where

$$\overline{\mathrm{Ra}}^* = \frac{\rho_a c_a \beta \Delta T g \bar{K}_= H}{\nu_a \bar{k}_{m\perp}} \tag{37}$$

is an overall Rayleigh number for the system, based on values of the mean parallel permeability and perpendicular thermal conductivity. The ratio of the longitudinal advected heat flux to the conducted heat flux perpendicular to the boundaries is:

$$\bar{q}_{hr} = \frac{\rho_a c_a q_{SS}}{\bar{k}_{m\perp}} \left[\frac{1}{H} \int_0^H \frac{K(z)}{\bar{K}_=} \left(\frac{1}{H} \int_z^H \frac{\bar{k}_{m\perp} d\zeta}{k_m(\zeta)} \right) dz \right] + \overline{\mathrm{Ra}}^* \sin\alpha \frac{1}{H} \int_0^H \left\{ \frac{K(z)}{\bar{K}_=} \left(\frac{1}{H} \int_z^H \frac{\bar{k}_{m\perp} d\zeta}{k_m(\zeta)} \right) \left[\frac{1}{H} \int_z^H \frac{\bar{k}_{m\perp} d\zeta}{k_m(\zeta)} - \frac{1}{H} \int_0^H \frac{K(\xi)}{\bar{K}_=} \left(\frac{1}{H} \int_\xi^H \frac{\bar{k}_{m\perp} d\zeta}{k_m(\zeta)} \right) d\xi \right] \right\} dz \tag{38}$$

Note that the usual formula for the Rayleigh number when considering instability of such a system is

$$\overline{\mathrm{Ra}}_\perp = \frac{\rho_a c_a \beta \Delta T g \bar{K}_\perp H}{\nu_a \bar{k}_{m\perp}} = \frac{\bar{K}_\perp}{\bar{K}_=} \overline{\mathrm{Ra}}^* = \frac{1}{\xi} \overline{\mathrm{Ra}}^* \tag{39}$$

where $\xi = \bar{K}_= / \bar{K}_\perp$ is the overall average permeability anisotropy of the layered permeable system, expressed as the ratio of the average parallel permeability to the perpendicular value, the latter being defined by

$$\int_0^H \frac{dz}{K(z)} = \frac{H}{\bar{K}_\perp}$$

3.4 Maximising advected heat

An interesting question is: What are the permeability and/or thermal conductivity distributions that maximize the advected heat flux in a naturally convective system? The "forced" convective component depends on q_{SS}, but the remainder depends on the counterflow induced by the temperature gradient across the sloping system. First, an investigation is made for uniform conductivity, then uniform permeability; these are followed by the most general case. While there may not be practical application to groundwater aquifers in the last case, the results could be useful for other system designs. This has a practical use in allowing a cap to be placed on the maximum advected flux along the layer.

Uniform thermal conductivity

In groundwater systems, the thermal conductivity does not vary very much. Assuming that $k_m(z) = k_m$, a constant, then, from (38):

$$q_{hr} = \frac{\rho_a c_a q_{SS}}{k_m} I_1 + \overline{\mathrm{Ra}}^* \sin\alpha \, (I_2 - I_1^2) \tag{40}$$

where

$$I_1 = \frac{1}{H}\int_0^H \frac{K(z)}{\bar{\bar{K}}_=}\left(1-\frac{z}{H}\right)dz = \int_0^1 (1-\zeta)\kappa(\zeta)d\zeta$$
$$I_2 = \frac{1}{H}\int_0^H \frac{K(z)}{\bar{\bar{K}}_=}\left(1-\frac{z}{H}\right)^2 dz = \int_0^1 (1-\zeta)^2\kappa(\zeta)d\zeta \qquad (41)$$

are (dimensionless) moments of the permeability distribution about the top boundary.

Here, $$\kappa(\zeta) = \frac{K(\zeta H)}{\bar{\bar{K}}_=}$$

is the non-dimensionalised permeability, with

$$\int_0^1 \kappa(\zeta)d\zeta = 1$$

From (40), the ratio of the naturally-convected heat flux to the conducted heat flux is found (by setting $q_{SS} = 0$) to be $\overline{\mathrm{Ra}}^* \sin\alpha\, J\{\kappa\}$, where $J\{\kappa\} = I_2 - I_1^2$. For uniform permeability (as well as conductivity), $\kappa(\zeta) = 1$, $J = 1/12$ and the ratio is $q_{hr} = (1/12)\ \mathrm{Ra}\ \sin\alpha$ where Ra is defined in (31). The more general problem is to seek the maximum possible value of the functional *J*, by finding the function $\kappa(\zeta)$ that gives this maximum value subject to the requirements:

$$\kappa(\zeta) \geq 0, \quad \int_0^1 \kappa(\zeta)d\zeta = 1 \qquad (42)$$

As shown in the Appendix, $J_{\max} = 3/20$, corresponding to permeability, temperature and fluid speed distributions:

$$\kappa(\zeta) = g(2\zeta-1) = 3(2\zeta-1)^2 + \sum_{n=3}^{\infty} c_n P_n(2\zeta-1)$$
$$T_{SS}(z) = T_a + \Delta T\left(1-\frac{z}{H}\right) \qquad (43)$$
$$u_{SS}(z) = \frac{\rho_a g\beta\Delta T\bar{\bar{K}}_=}{2\mu_a}\sin\alpha\left(1-\frac{2z}{H}\right)\left[3\left(1-\frac{2z}{H}\right)^2 + \sum_{n=3}^{\infty} c_n P_n\left(\frac{2z}{H}-1\right)\right]$$

where $P_n(\theta)$ is the Legendre polynomial of order *n*, defined on $-1 \leq \theta \leq 1$, and the coefficients c_n $(n \geq 3)$ must be chosen so that $\kappa(\zeta) \geq 0$ for $\zeta \in [0,1]$. The case where $q_{SS} = 0$, $c_n = 0$ $(n \geq 3)$ is shown in Figure 4.

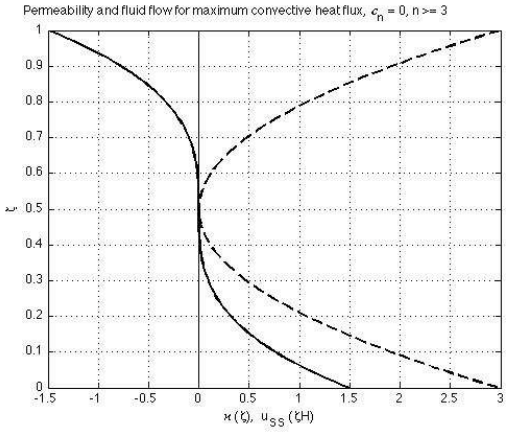

Figure 4. Permeability distribution $\kappa(\zeta)$ (dashed line) and consequent fluid Darcy speed profile (solid line) for optimal advected heat in a layer where the thermal conductivity is uniform.

There is one intriguing aspect. While the maximum value of the integral now seems fixed, there remains some arbitrariness for the permeability function as given in (43). As stated above, the only constraint on the c_n, $n \geq 3$, is that $\kappa(\zeta) \geq 0$ in [0, 1]. Two examples, where P_4 is non-zero, are shown in Figure 5, with $c_4 = 2$ and 3 respectively. The solution when $c_4 = 3$ is inadmissible as the permeability function then becomes negative for some values of ζ. Note that, in both cases, the advective heat transfer along the aquifer is the same as in Figure 4.

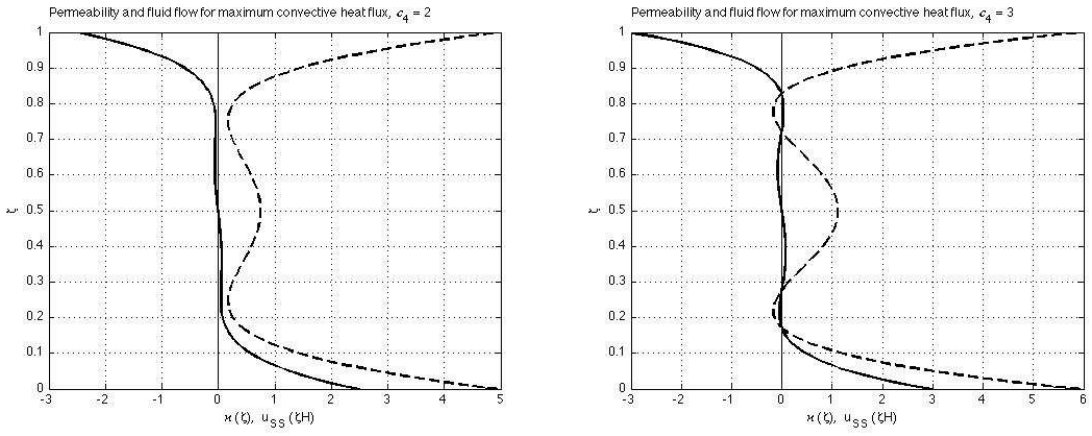

Figure 5. Permeability (dashed lines) and fluid Darcy speed profiles (solid lines) for $c_4 = 2$ (left) and $c_4 = 3$ (right).

Uniform permeability

Assuming that $K(z) = K$, a constant, then, from (38):

$$\bar{q}_{hr} = \frac{\rho_a c_a q_{SS}}{\bar{k}_{m\perp}} I_3 + \overline{\mathrm{Ra}}^* \sin\alpha \; (I_4 - I_3^{\,2}) \tag{44}$$

where

$$\begin{aligned} I_3 &= \frac{1}{H}\int_0^H \left(\frac{1}{H}\int_z^H \frac{\bar{k}_{m\perp} d\zeta}{k_m(\zeta)} \right) dz = \int_0^1 \left(\int_\zeta^1 \frac{d\xi}{\chi(\xi)} \right) d\zeta \\ I_4 &= \frac{1}{H}\int_0^H \left(\frac{1}{H}\int_z^H \frac{\bar{k}_{m\perp} d\zeta}{k_m(\zeta)} \right)^2 dz = \int_0^1 \left(\int_\zeta^1 \frac{d\xi}{\chi(\xi)} \right)^2 d\zeta \end{aligned} \tag{45}$$

Here, $\chi(\xi) = k_m(\xi H)/\bar{k}_{m\perp}$ is the non-dimensionalised thermal conductivity, with $\int_0^1 \frac{d\xi}{\chi(\xi)} = 1$.

The maximum heat transfer ratio for natural convection ($q_{SS} = 0$) is determined by finding the thermal conductivity distribution $\chi(\zeta)$ that maximizes the functional $J\{\chi\} = I_4 - I_3^{\,2}$ [see (44)]. As shown in the Appendix, $J_{\max} = 1/4$, with the corresponding optimal thermal conductivity, temperature and fluid speed distributions given by

$$\begin{aligned} \int_{z/H}^1 \frac{d\zeta}{\chi(\zeta)} &= 1 - \mathcal{H}\left(\frac{z}{H} - \frac{1}{2}\right) \\ \frac{\bar{k}_{m\perp}}{k_m(z)} &= \delta\left(\frac{z}{H} - \frac{1}{2}\right) \\ T_{SS}(z) &= T_a + \Delta T\left[1 - \mathcal{H}\left(\frac{z}{H} - \frac{1}{2}\right)\right] \\ u_{SS}(z) &= \frac{\rho_a g \beta \Delta T \bar{K}_=}{\mu_a} \sin\alpha \left[\frac{1}{2} - \mathcal{H}\left(\frac{z}{H} - \frac{1}{2}\right)\right] \end{aligned} \tag{46}$$

where $\mathcal{H}(\zeta)$ is the Heaviside (step) function. Alternatively, these may be written:

$$\begin{aligned} T_{SS}(z) &= \begin{cases} T_a + \Delta T, & 0 \le z < \dfrac{H}{2} \\ T_a, & \dfrac{H}{2} < z \le 1 \end{cases} \\ u_{SS}(z) &= \begin{cases} +\dfrac{\rho_a g \beta \Delta T \bar{K}_=}{2\mu_a} \sin\alpha, & 0 \le z < \dfrac{H}{2} \\ -\dfrac{\rho_a g \beta \Delta T \bar{K}_=}{2\mu_a} \sin\alpha, & \dfrac{H}{2} < z \le 1 \end{cases} \end{aligned} \tag{47}$$

These (physically, somewhat bizarre) profiles correspond to uniform temperature $T_{SS} = T_a + \Delta T$ in the lower half of the aquifer, where the thermal conductivity is infinite, while $T_{SS} = T_a$ in the upper half, again with infinite conductivity. The conductivity at $z = H/2$ is briefly zero on an infinitely thin planar region, which separates the lower up-slope flow from the down-slope flow above (both relative to the nett flow caused by forced fluid convection).

General case

It is also possible to maximize the heat flux ratio for arbitrary permeability and conductivity. The problem is formulated in the Appendix. Again, the functional maximum is found to be $1/4$. But there is some arbitrariness for the permeability distribution, as found above for the constant thermal conductivity case.

3.5 Layered system

From (20) and (21), the piecewise-linear temperature and fluid flux profiles for Layer *j* are:

$$T_{SSj}(z) = T_a + \Delta T\left[1 - \left(\sum_{i=1}^{j-1}\frac{\eta_i}{\chi_i} + \frac{(z - z_{j-1})/H}{\chi_j}\right)\right]$$

$$u_{SSj}(z) = \kappa_j \frac{q_{SS}}{H} + \frac{\rho_a \beta \Delta T g \bar{K}_=}{\mu_a}\sin\alpha\ \kappa_j\left\{\sum_{r=1}^{N}\left[\eta_r\kappa_r\left(\sum_{i=1}^{r-1}\frac{\eta_i}{\chi_i} + \frac{\eta_r}{2\chi_r}\right)\right] - \left(\sum_{i=1}^{j-1}\frac{\eta_i}{\chi_i} + \frac{(z - z_{j-1})/H}{\chi_j}\right)\right\}$$

Then the (constant) conducted heat is

$$\bar{q}_{h\perp} = -k_m(z)\frac{dT_{SS}}{dz} = -k_{m1}\frac{dT_{SS1}}{dz}(0) = \bar{k}_{m\perp}\frac{\Delta T}{H} \tag{48}$$

and the net convected flux is

$$\begin{aligned}\bar{q}_{h=} &= \frac{1}{H}\int_0^H \rho_a c_a [T_{SS}(z) - T_a] u_{SS}(z)dz = \frac{1}{H}\sum_{j=1}^{N}\left[\int_{z_{j-1}}^{z_j} \rho_a c_a [T_{SSj}(z) - T_a] u_{SSj}(z)dz\right] \\ &= \bar{k}_{m\perp}\frac{\Delta T}{H}\frac{\rho_a c_a q_{SS}}{\bar{k}_{m\perp}}\left[\sum_{j=1}^{N}\kappa_j\eta_j\left(1 - \sum_{i=1}^{j-1}\frac{\eta_i}{\chi_i} - \frac{\eta_j}{2\chi_j}\right)\right] \\ &\quad + \bar{k}_{m\perp}\frac{\Delta T}{H}\ \overline{\mathrm{Ra}^*}\sin\alpha\ \sum_{j=1}^{N}\kappa_j\eta_j\left\{\begin{array}{l}\left[1 - \sum_{i=1}^{j-1}\frac{\eta_i}{\chi_i}\right]\left[\sum_{r=1}^{N}\eta_r\kappa_r\left(\sum_{i=1}^{r-1}\frac{\eta_i}{\chi_i} + \frac{\eta_r}{2\chi_r}\right) - \sum_{i=1}^{j-1}\frac{\eta_i}{\chi_i}\right] \\ -\frac{\eta_j}{2\chi_j}\left[\sum_{r=1}^{N}\eta_r\kappa_r\left(\sum_{i=1}^{r-1}\frac{\eta_i}{\chi_i} + \frac{\eta_r}{2\chi_r}\right) - \sum_{i=1}^{j-1}\frac{2\eta_i}{\chi_i} + 1\right] + \frac{\eta_j^{\,2}}{3\chi_j^{\,2}}\end{array}\right\}\end{aligned} \tag{49}$$

As a check, when all the layer permeabilities and thermal conductivities are the same (i.e., $\kappa_j = \chi_j = 1$, $j = 1, \ldots, N$), it can be shown that this reduces to the result for a single layer given by (28), as expected.

4. SUMMARY & CONCLUSIONS

This paper describes some simple mathematical models that can be used to compute the velocity profiles and the heat flux advected by a fluid flowing within a permeable matrix. The groundwater systems have (parallel) layered structures and the linear advection-dispersion equations that model the transport have coefficients that depend mainly on depth. A temperature difference between the lower and upper boundaries of a sloping system induces a counterflow closely aligned to the slope; this flow is stable provided the system Rayleigh number is not too large. (Full quantification of the criteria for stability of such a counterflow are beyond the ambit of this paper, but the investigation is underway and results will be available in due course.)

The parameters that contribute to the coefficients in the partial differential equations are assumed constant within each layer, but can be different in each of the various layers. The resulting linear constant-coefficient pde's are coupled by temperature and heat flux continuity requirements at the layer interfaces.

The maximum ratio of the nett naturally-advected heat parallel to the aquifer to the conducted heat perpendicular to the boundaries has been calculated for the two cases where the thermal conductivity and the permeability are uniform while the other varies, and also the more general case where neither profile is pre-determined. The three maximum ratios are, respectively: $q_{hr\,\max} = (3/20,\ 1/4,\ 1/4)\ \overline{\mathrm{Ra}}^*\ \sin\alpha$, where the various parameters have been defined above.

Caltagirone & Bories (1985) found that the parallel flow in a sloping homogeneous layer was stable to longitudinal rolls with their axes parallel to the slope provided $\mathrm{Ra}\ \cos\alpha < 4\pi^2$. Earlier, Epherre (1985) had found that for a horizontal layer where the permeability and thermal conductivity were uniform and anisotropic, the critical Rayleigh number for onset of convection in the form of rolls, minimized over cell width/depth ratio is, in terms of notation used here,

$$\overline{\mathrm{Ra}}_{\perp\mathrm{crit}} = \pi^2 \left[1 + \sqrt{\eta/\xi} \right]^2 .$$

where $\xi = \bar{K}_{=} / \bar{K}_{\perp}$ and $\eta = \bar{k}_{m=} / \bar{k}_{m\perp}$ are the measures of large-scale average anisotropy in permeability and conductivity respectively. If it is assumed that the anisotropic result can be carried over to a sloping layer, then flow parallel to a uniformly anisotropic sloping slab will be stable provided $\overline{\mathrm{Ra}}_{\perp} \cos\alpha < \pi^2 \left[1 + \sqrt{\eta/\xi} \right]^2$. Using (39), this criterion for stability becomes:

$$\overline{\mathrm{Ra}}^{*} \cos\alpha = \xi \, \overline{\mathrm{Ra}}_{\perp} \cos\alpha < \pi^2 \left[\sqrt{\xi} + \sqrt{\eta} \right]^2$$

Then, the values of the heat flow ratios, while the parallel counterflow persists, are constrained by:

$$q_{hr\,\max} < (3/20,\ 1/4,\ 1/4)\, \pi^2 \tan\alpha \left[\sqrt{\xi} + \sqrt{\eta} \right]^2$$

respectively for the cases of uniform thermal conductivity, uniform permeability and general distributions. So, while the system acts like a heat pipe, the heat advected by natural convection is relatively small for homogeneous systems with small slope, but may be larger for anisotropic systems or those with larger slope, provided conditions for stability remain satisfied.

McKibbin & Tyvand (1982) found that, for a horizontal system composed of alternating layers of two different thicknesses, permeability and thermal conductivity, a single equivalent homogeneous anisotropic layer was a suitable analogy for the periodic system, in terms of stability of the initial motionless flow, the cell aspect ratio at onset of convection and consequent heat transfer at slightly supercritical conditions, provided the length scale of the flow is larger than the layering period. However, when the contrast in layer matrix properties is too great, stacks of small-scale convective cells may be induced, and the analogy breaks down. Interestingly, they report that, when the layers have the same thermal conductivity but a contrast in permeability that is severe enough to favour such small-scale convection, the "mixed" Rayleigh number:

$$\overline{\mathrm{Ra}}^{*} = \frac{\rho_a c_a \beta \Delta T g \bar{K}_{=} H}{\nu_a \bar{k}_{m\perp}},$$

as defined in (37) above and with $\bar{k}_{m\perp} = k_m$ (uniformly constant), has a critical value that is nearly independent of the permeability anisotropy ratio ξ. Such relationships will be investigated as further work on the stability criteria for sloping layered systems continues.

In natural groundwater systems within geothermally-heated regions of the Earth's crust, it is of interest to know whether conditions that promote natural convection in sloping aquifers exist. If

so, there may be some heat transfer parallel to the bedding plane that could be usefully-exploited. However, of more interest may be the transport of pollutants and/or tracers by the flow; the present work indicates that the direction of such transport would depend strongly on the depth at which any species is injected. Quantification of such transport depends on using the fluid flow profiles, as established above, and advection-dispersion equations to describe the motion of a pollutant, as in McKibbin (2009). This work is underway and will be reported soon.

ACKNOWLEDGEMENT

The contribution of the second and third authors, Nick Hale and Robert Style, was supported by Award No. KUK-C1-013-04, made by King Abdullah University of Science and Technology (KAUST).

APPENDIX

Uniform thermal conductivity

The problem is to find the function $\kappa(\zeta)$ that maximizes the functional

$$J\{\kappa\} = \int_0^1 \left(1-\zeta\right)^2 \kappa(\zeta)\, d\zeta - \left[\int_0^1 \left(1-\zeta\right)\kappa(\zeta)\, d\zeta\right]^2 \tag{A1}$$

subject to the requirements:

$$\kappa(\zeta) \geq 0, \quad \int_0^1 \kappa(\zeta)\, d\zeta = 1$$

The standard methods of the variational calculus are unable to applied. Instead, $\kappa(\zeta)$ is written in terms of Legendre polynomials:

$$\kappa(\zeta) = f(2\zeta - 1) = f(\theta) = \sum_{n=0}^{\infty} c_n P_n(\theta) \tag{A2}$$

where the $P_n(\theta)$, $n \geq 0$, are orthogonal on the domain [–1, 1], with $\int_{-1}^{1} P_m(\theta) P_n(\theta)\, d\theta = \frac{2}{2n+1}\delta_{mn}$.

Since $P_0(\theta)=1$, we have $\int_{-1}^{1} P_0(\theta)d\theta = 2$, and $\int_{-1}^{1} P_n(\theta)d\theta = 0$ for $n \geq 1$. We may then write the functional to be maximized as:

$$\begin{aligned}\hat{J}\{f\} &= \int_{-1}^{1}\left(\frac{\theta+1}{2}\right)^2 f(\theta)\frac{1}{2}d\theta - \left(\int_{-1}^{1}\frac{\theta+1}{2}f(\theta)\frac{1}{2}d\theta\right)^2 \\ &= \frac{1}{8}\int_{-1}^{1}\theta^2 f(\theta)d\theta - \frac{1}{16}\left(\int_{-1}^{1}\theta f(\theta)d\theta\right)^2\end{aligned} \tag{A3}$$

Now, $P_0(\theta)=1$, $P_1(\theta)=\theta$, $P_2(\theta)=\frac{1}{2}(3\theta^2-1)$, so $\theta = P_1(\theta)$, $\theta^2 = \frac{1}{3}[P_0(\theta)+2P_2(\theta)]$, and

$$\begin{aligned}\hat{J}\{f\} &= \frac{1}{8}\int_{-1}^{1}\theta^2 f(\theta)d\theta - \frac{1}{16}\left(\int_{-1}^{1}\theta f(\theta)d\theta\right)^2 \\ &= \frac{1}{8}\int_{-1}^{1}\frac{1}{3}[P_0(\theta)+2P_2(\theta)]\sum_{0}^{\infty}c_n P_n(\theta)d\theta - \frac{1}{16}\left(\int_{-1}^{1}P_1(\theta)\sum_{0}^{\infty}c_n P_n(\theta)d\theta\right)^2 \\ &= \frac{1}{12}c_0 + \frac{1}{30}c_2 - \frac{1}{36}c_1^{\,2}\end{aligned}$$

using the orthogonality. This is maximized when $c_1 = 0$; then

$f(\theta) = c_0 + c_2\,\frac{1}{2}(3\theta^2-1) + \sum_{n=3}^{\infty}c_n P_n(\theta)$. We also have $\int_{0}^{1}\kappa(\zeta)d\zeta = \int_{-1}^{1}f(\theta)\frac{1}{2}d\theta = 1$, so $\int_{-1}^{1}f(\theta)d\theta = 2$, which gives $c_0 = 1$. The non-negativity condition, that $\kappa(\zeta) = f(\theta) \geq 0$ whatever the values of c_n, $n \geq 3$, implies that $c_2 \leq 2$. So, taking $c_2 = 2$, the maximum value of J is:

$$J_{\max} = \hat{J}_{\max} = \frac{1}{12}(1) + \frac{1}{30}(2) - \frac{1}{36}(0)^2 = \frac{3}{20} \tag{A4}$$

Uniform permeability

The problem is to find the function $\chi(\zeta)$ that maximizes the functional $J\{\chi\}$ defined by:

$$J\{\chi\} = \int_0^1\left(\int_\zeta^1\frac{d\xi}{\chi(\xi)}\right)^2 d\zeta - \left[\int_0^1\left(\int_\zeta^1\frac{d\xi}{\chi(\xi)}\right)d\zeta\right]^2 \tag{A5}$$

subject to the requirements:

$$\chi(\zeta) \geq 0, \quad 0 \leq G(\zeta) = \int_{\zeta}^{1} \frac{d\xi}{\chi(\xi)} \leq 1, \quad G(0) = \int_{0}^{1} \frac{d\xi}{\chi(\xi)} = 1$$

Write:

$$g(\theta) = g(2\zeta - 1) = 2G(\zeta) - 1 = 2\int_{\zeta}^{1} \frac{d\xi}{\chi(\xi)} - 1 \tag{A6}$$

which is a monotonic decreasing function of θ with $g(-1) = 1,\ g(1) = -1$. Then:

$$\begin{aligned} J\{\chi\} &= \hat{J}\{G\} \\ &= \frac{1}{8}\int_{-1}^{1} [g(\theta)]^2 d\theta - \frac{1}{16}\left[\int_{-1}^{1} g(\theta) d\theta\right]^2 \end{aligned} \tag{A7}$$

where $-1 \leq g(\theta) \leq 1$. The first term is a maximum when $g(\theta) = \pm 1$. The second achieves its minimum value when $\int_{-1}^{1} g(\theta) d\theta = 0$. Also, $g(-1) = 1,\ g(1) = -1$. All conditions are satisfied, and the functional maximized, with a value of $J_{\max} = 1/4$ when:

$$g(\theta) = 1 - 2\mathcal{H}(\theta) \tag{A8}$$

on $-1 \leq \theta \leq 1$. In terms of the original functions:

$$\begin{aligned} G(\zeta) &= \frac{1}{2}\left[1 + g(2\zeta - 1)\right] = 1 - \mathcal{H}(\zeta - \frac{1}{2}) \\ \int_{0}^{\zeta} \frac{d\xi}{\chi(\xi)} &= \mathcal{H}(\zeta - \frac{1}{2}) \\ \frac{1}{\chi(\zeta)} &= \delta(\zeta - \frac{1}{2}) \end{aligned} \tag{A9}$$

This corresponds to infinite thermal conductivity across the aquifer except for an infinitely thin band of zero conductivity at $z = H/2$.

General case

Writing $G(\zeta) = \int_{\zeta}^{1} \frac{d\xi}{\chi(\xi)}$ as above, then from (38) with $q_{SS} = 0$:

$$\bar{q}_{hr} = \frac{\bar{q}_{h\rightleftharpoons}}{q_{h\perp}} = \overline{\mathrm{Ra}}^{*} \sin\alpha \left[\int_0^1 \kappa(\zeta) G^2(\zeta) d\zeta - \left(\int_0^1 \kappa(\zeta) G(\zeta) d\zeta \right)^2 \right] \tag{A10}$$

with constraints:

$$\begin{aligned} &\kappa(\zeta) \geq 0, \quad \int_0^1 \kappa(\zeta) d\zeta = 1, \\ &G(0) = 1, \quad G(1) = 0, \\ &G'(\zeta) \leq 0, \; G(\zeta) \in [0,1] \quad \textit{for} \quad \zeta \in [0,1]. \end{aligned} \tag{A11}$$

To optimize the heat flux ratio we must maximize the functional

$$J\{\kappa, G\} = \int_0^1 \kappa(\zeta) G^2(\zeta) d\zeta - \left(\int_0^1 \kappa(\zeta) G(\zeta) d\zeta \right)^2 \tag{A12}$$

subject to the constraints (A11). Writing $\theta = 2\zeta - 1$, and defining $f(\theta) = \kappa(\zeta)$, $g(\theta) = 2G(\zeta) - 1$, as before, the problem is equivalent to maximizing the functional

$$\hat{J}\{f, g\} = \frac{1}{8} \int_{-1}^1 f(\theta) g^2(\theta) d\theta - \frac{1}{16} \left(\int_{-1}^1 f(\theta) g(\theta) d\theta \right)^2 \tag{A13}$$

subject to:

$$\begin{aligned} &f(\theta) \geq 0, \quad \int_{-1}^1 f(\theta) d\theta = 2, \\ &g(-1) = 1, \; g(1) = -1, \\ &g'(\theta) \leq 0, \; g(\theta) \in [-1,1] \quad \textit{for} \quad \theta \in [-1,1]. \end{aligned} \tag{A14}$$

The first term on the RHS of (A13) is always non-negative, and the second term is clearly non-positive. The maximum value the functional can take is when the first term is maximized and the second is zero. The integrand in the first term is non-negative and we make this as large as possible at every point in the domain of definition. Regardless of the form of $f(\theta)$, this can only be achieved if $g^2(\theta)$ takes its largest possible value everywhere; because of the third constraint, this means $g(\theta) = \pm 1$. With the other requirements on *g* as in (A14), the optimal function g^* must take the form of a shifted sign function:

$$g^*(\theta) = -\mathrm{sgn}(\theta - c^*) = 1 - 2\mathcal{H}(\theta - c^*) \tag{A15}$$

where c^* is a constant in the range $(-1,1)$ but, so far, otherwise arbitrary. Substitution of g^* into the functional and use of the constraint on the integral of f from (A14) gives:

$$\begin{aligned}\hat{J}\{f,g^*\} &= \frac{1}{8}\int_{-1}^{1} f(\theta)d\theta - \frac{1}{16}\left(\int_{-1}^{c^*} f(\theta)d\theta - \int_{c^*}^{1} f(\theta)d\theta\right)^2 \\ &= \frac{1}{4} - \frac{1}{16}\left(\int_{-1}^{c^*} f(\theta)d\theta - \int_{c^*}^{1} f(\theta)d\theta\right)^2\end{aligned} \tag{A16}$$

So, any function f^* satisfying

$$\begin{aligned}&\int_{-1}^{c^*} f^*(\theta)d\theta = \int_{c^*}^{1} f^*(\theta)d\theta, \\ &f^*(\theta) \geq 0, \qquad \int_{-1}^{1} f^*(\theta)d\theta = 2,\end{aligned} \tag{A17}$$

will maximize the functional J, with

$$J_{\max} = \hat{J}(f^*,g^*) = \frac{1}{4} \tag{A18}$$

Even for a fixed value of $c^* \in (-1,1)$, there may be an infinite number of solutions for $f^*(\theta)$. One such solution is the linear function

$$f^*_{\text{linear}}(\theta) = 1 + \frac{2c^*}{1-c^{*2}}\theta,$$

Then $\kappa^*_{\text{linear}}(\zeta) = f^*_{\text{linear}}(2\zeta - 1) = 1 - \frac{2c^*}{1-c^{*2}} + \frac{4c^*}{1-c^{*2}}\zeta$. In this case, the non-negativity constraint on $\kappa(0) = f(-1)$ requires that $c^* \in (-1, \sqrt{2}-1)$.

If the permeability is constant, $f(\theta) = 1$ and $c^* = 0$; the unique $g^*(\theta)$ for which $\hat{J}(1,g^*) = 1/4$ is $g^*(\theta) = -\text{sgn}(\theta) = 1 - 2\mathcal{H}(\theta)$. Physically, this corresponds to infinite thermal conductivity across the aquifer except for an infinitely-thin band of zero conductance at $z = H/2$.

REFERENCES

Bories, S.A. and Combarnous, M.A., Natural convection in a sloping porous layer, J. Fluid Mech., vol. 57, pp. 63-79, 1973.

Caltagirone, J.P. and Bories, S., Solutions and stability criteria of natural convective flow in an inclined porous layer, J. Fluid Mech., vol. 155, pp. 267-287, 1985.

Horton, C.W. and Rogers, F.T., Convection currents in a porous medium, J. Appl. Phys., vol. 16, pp. 367-370, 1945.

Lapwood, E.R., Convection of a fluid in a porous medium, Proc. Camb. Phil. Soc., vol. 44, pp. 508-521, 1948.

Lim, L.L., Sweatman, W.L. and McKibbin, R., A simple deterministic model for volcanic ashfall deposition, The ANZIAM Journal, vol. 49, pp. 325-336, 2008.

Ludvigsen, A., Palm, E. and McKibbin, R., Convective momentum and mass transport in porous sloping layers, J. Geophys. Res., vol. 97, pp. 12315-12325, 1992.

McKibbin, R., Convection and heat transfer in layered and anisotropic porous media. In Quintard, M. and Todorovic, M., Heat and mass transfer in porous media, Elsevier, Amsterdam, pp. 327-336, 1992.

McKibbin, R., Mathematical modelling of aerosol transport and deposition: Analytic formulae for fast computation. In Proc. iEMSs Fourth Biennial Meeting, International Congress on Environmental Modelling and Software (iEMSs 2008), Barcelona, Spain, 7 – 10 July 2008, iEMSs, pp. 1420-1430, 2008.

McKibbin, R., Groundwater pollutant transport: transforming layered models to dynamical systems. In An. St. Univ. Ovidius Constanta, Serie Matematica, vol. 17, part 3, Ovidius University of Constantza, pp. 183-196, 2009.

McKibbin, R. and O'Sullivan, M.J., Heat transfer in a layered porous medium heated from below, J. Fluid Mech., vol. 111, pp. 141-173, 1981.

McKibbin, R. and Tyvand, P.A., Anisotropic modeling of thermal convection in multilayered porous media, J. Fluid Mech., vol. 118, pp. 315-339, 1982.

Mullis, A.M., Natural convection in porous, permeable media: sheets, wedges and lenses, Marine and Petroleum Geology, vol. 12, pp. 17-25, 1995.

Nield, D.A. and Bejan, A., Convection in Porous Media (3rd edition), Springer-Verlag, New York, 2006.

Trew, M. and McKibbin, R., Convection in anisotropic inclined porous layers, Transp. Porous Media, vol. 17, pp. 271-283, 1994.

RECENT REPORTS

16/10	The Physics and Mechanics of Biological Systems	Goriely Moulton
17/10	Crust formation in drying colloidal suspensions	Style Peppin
18/10	A Mathematical Model of Tumor-Immune Interactions	Robertson-Tessi El-Kareh Goriely
19/10	Elastic cavitation, tube hollowing, and differential growth in plants and biological tissues	Goriely Moulton Vandiver
20/10	Asymptotic expressions for the nearest and furthest dislocations in a pile-up against a grain boundary	Hall
21/10	Cardiac electromechanics: the effect of contraction model on the mathematical problem and accuracy of the numerical scheme	Pathmanathan Chapman Gavaghan Whiteley
22/10	Fat vs. thin threading approach on GPUs: application to stochastic simulation of chemical reactions	Klingbeil Erban Giles Maini
23/10	Asymptotic analysis of a system of algebraic equations arising in dislocation theory	Hall Chapman Ockendon
25/10	Preconditioning for Allen-Cahn Variational Inequalities with Non-Local Constraints	Blank Sarbu Stoll
26/10	On an evolution equation for sand dunes	Ellis Fowler
27/10	On Liquid Films on an Inclined Plate	Benilov Chapman McLoed Ockendon Zubkov
28/10	An a posteriori error analysis of a mixed finite element Galerkin approximation to second order linear parabolic problems	Memon Nataraj Pani
29/10	A Priori Error Estimates for Semidiscrete Finite Element Approximations to Equations of Motion Arising in Oldroyd Fluids of Order One	Goswami Pani
30/10	The Landau-de Gennes theory of nematic liquid crystals: Uniaxiality versus Biaxiality	Majumdar
31/10	The Radial-Hedgehog Solution in Landau-de Gennes' theory	Majumdar

32/10	Nonlinear instability in flagellar dynamics: a novel modulation mechanism in sperm migration?	Gadelha Gaffney Smith Kirkman-Brown
33/10	Error bounds on block GaussSeidel solutions of coupled multi-physics problem	Whiteley Gillow Tavener Walter
34/10	A random projection method for sharp phase boundaries in lattice Boltzmann simulations	Reis Dellar
35/10	Regularized Particle Filter with Langevin Resampling Step	Duan Farmer Moroz
36/10	Sequential Inverse Problems Bayesian Principles and the Logistic Map Example	Duan Farmer Moroz
37/10	Circumferential buckling instability of a growing cylindrical tube	Moulton Goriely
38/10	Preconditioners for state constrained optimal control problems with Moreau-Yosida penalty function	Stoll Wathen
39/10	Local synaptic signaling enhances the stochastic transport of motor-driven cargo in neurons	Newby Bressloff

Copies of these, and any other OCCAM reports can be obtained from:

Oxford Centre for Collaborative Applied Mathematics
Mathematical Institute
24 - 29 St Giles'
Oxford
OX1 3LB
England
www.maths.ox.ac.uk/occam